



γ production in neutrino interactions with nucleiG. Chanfray ¹ and M. Ericson ^{1,2}¹*Univ. Lyon, Univ. Claude Bernard Lyon 1, CNRS/IN2P3, IP2I Lyon, UMR 5822, F-69622, Villeurbanne, France*²*Theory division, CERN, CH-12111 Geneva, Switzerland*

(Received 6 May 2021; accepted 6 July 2021; published 26 July 2021)

We evaluate the cross section for gamma production by neutrinos through a meson exchange effect which derives from the concept of axial-vector mixing. The resulting cross section leads to some increase of the gamma production cross section by neutrinos, especially at low neutrino energies, which may influence the understanding of the low-energy excess of electron-like events seen in the MiniBooNE experiment.

DOI: [10.1103/PhysRevC.104.015203](https://doi.org/10.1103/PhysRevC.104.015203)**I. INTRODUCTION**

The problem of gamma emission in the interaction of neutrinos with nuclei is of great interest for the interpretation of the low-energy excess of electron-like events seen in the MiniBooNE experiment [1,2]. In this short baseline (541 m) muon neutrino primary beam experiment a number of low-energy electrons have been detected in the target. The shortness of the baseline excluding oscillations into the known neutrinos, this observation has been interpreted as evidence for a new neutrino, the sterile neutrino, more massive than the known neutrinos and whose existence has been vividly discussed. This anomalous excess has been confirmed in a recent analysis [3]. The importance of this result has triggered a number of investigations to explore alternative interpretations for the presence of these electrons. A possibility is that gamma rings produced in the target have been mistaken for electron rings, as the MiniBooNE detector cannot distinguish the two, thus artificially increasing the apparent number of electrons. It is therefore crucial to have a proper evaluation of the gamma emission background in the interaction of neutrinos.

Several evaluations of this process have been made [4–9]. They involve in particular the production of a Delta, which decays by gamma emission. In these events where the gamma rings could be mistaken for electrons, no lepton are emitted and the process for gamma production involves a neutral current transition: the vector boson Z_0 in its interaction with a nucleon excites a Delta which emits a photon, as shown in Fig. 1(a). However, even if all these photons are mistaken for electrons this process has not been able to account for the observed number of electrons without a sterile neutrino oscillation [10].

In this work we introduce another source for gamma production by neutrinos which, to our knowledge, has not been considered in connection with this problem. It involves a meson exchange effect from a contact vertex where, together with the gamma, a pion is produced at the $N\Delta$ vertex, as depicted on Fig. 1(b). The contact $\langle N|\pi\gamma|\Delta\rangle$ coupling is obtained from the usual p -wave coupling $\langle N|\partial_\nu\pi|\Delta\rangle$ by the minimal substitution where in short ∂_ν is replaced by $(\partial_\nu - qA_\nu)$. Its precise form is given below. In the interaction of real photons with a free nucleon this contact coupling is responsible for an appreciable part of the photon-nucleon cross section in the energy region above the Delta energy, $\omega \simeq 400\text{--}500$ MeV. Notice that the process of $\gamma\pi$ simultaneous production as such would not affect the MiniBooNE interpretation because the pion produced in this process is detectable, while instead in the selected events no pions are observed. However, in the nucleus the pion is dressed, in particular by particle-hole (ph) excitations, thus acquiring a broad spectrum which extends on the low-energy side of the pion mass. In the MiniBooNE detector which does not identify nuclear excitations, when a pion produced is disguised as a ph state it becomes invisible, simulating a simple gamma production process and contributing to an increase of the gamma emission cross section. The fact that the energy distribution of the process where the pion is materialized as a ph excitation is smaller than the one where it is emitted as a real pion is interesting because the apparent electron excess in MiniBooNE occurs below a reconstructed neutrino energy of approximately 400 MeV.

The introduction of the graph of Fig. 1(b) is not randomly chosen: it embodies the concept of axial-vector mixing in the nuclear medium introduced by Chanfray *et al.* [11]. This concept consists in the following: the s -wave absorption (or emission) by a nucleon (or a Delta) of a pion emitted by a neighboring nucleon, as illustrated in Fig. 1(b), produces a parity change which transforms a vector correlator into an axial one (or the reverse). It extends to the nuclear case the concept, introduced by Dey *et al.* [12], of parity mixing by the thermal pions of a heat bath. In the nuclear medium the virtual pions of the pionic clouds replace the thermal pions of

Published by the American Physical Society under the terms of the [Creative Commons Attribution 4.0 International](https://creativecommons.org/licenses/by/4.0/) license. Further distribution of this work must maintain attribution to the author(s) and the published article's title, journal citation, and DOI. Funded by SCOAP³.

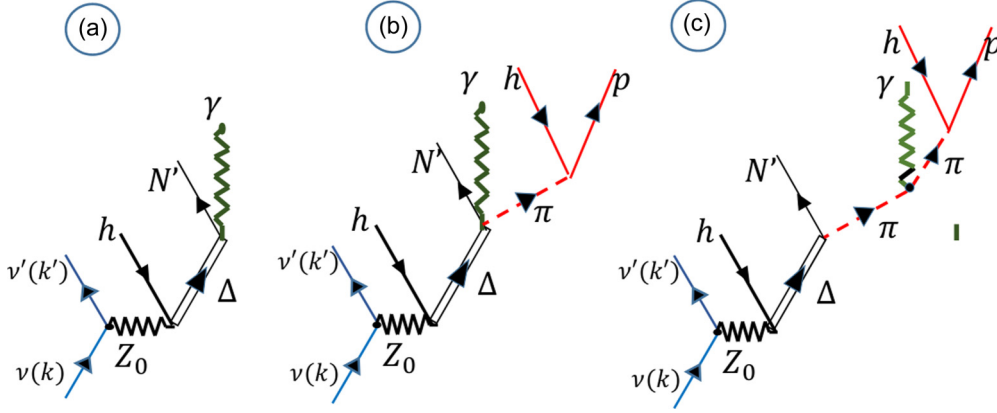


FIG. 1. (a) Single γ emission process considered in Refs. [4–9]. (b) Contact γ -pion emission process. (c) Pion in flight process.

the heat bath. Drawn in the perspective of correlator mixing the vector-vector correlator [graph 2(c) of Fig. 2 of Ref. [11]] is associated with the mixing ones represented by graphs 2(d)–2(f) of the same figure. As a side remark we also point out that the pion cloud contribution to the broadening of the rho meson observed in dilepton production in relativistic heavy-ion collisions [13,14] originates from such an axial-vector mixing effect, as demonstrated first in Ref. [11].

In the simpler case of the interaction of real photons with nuclei, the effect expected from the correlator mixing is a spreading of the gamma nucleus cross section due to the $\pi N\Delta$ contact term over a larger range of energy, increasing the nuclear cross section as compared with the nucleonic one in the low-energy transfer region, $\omega \leq 500$ MeV and producing some depletion above, in the energy region where the original $\pi N\Delta$ contact term acts. These features are remarkably similar to those of the MiniBooNE excess event but this analogy is premature because the kinematics of neutrino interactions is different. The contact $\pi N\Delta$ graph that we have discussed is not the only mixing term. There is also the one where the gamma is absorbed by a pion in flight, as shown in Fig. 1(c). We have also evaluated this term and it contributes significantly.

Summarizing, the aim of the present work is the evaluation of the cross section for the process of gamma emission on the ^{12}C nucleus by neutrinos through the contact $N\Delta\gamma\pi$ term, leading to a final 2p-2h excited state. We use for the ^{12}C nucleus a nuclear matter description with a typical density $\rho = 0.8\rho_0$, where ρ_0 is the normal nuclear matter density. The process which for a free nucleon is $Z_0 + N \rightarrow \Delta \rightarrow N\pi\gamma$ leads in the nucleus to $Z_0 + A \rightarrow \Delta(A-1) \rightarrow \gamma\pi 1p1h(A-1) \rightarrow \gamma 2p2h(A-2)$. As mentioned above, the final state, which consists of a gamma plus an (invisible) 2p-2h excitation can be mistaken for a gamma emission and hence for an electron emission process. This contribution is appreciably different in different neutrino energy regions, an interesting feature for the MiniBooNE experiment where the excess is concentrated in a region of neutrino energy below $\simeq 400$ MeV.

In the following we denote by $k = (E_\nu, \mathbf{k})$ and $k' = (E'_\nu, \mathbf{k}')$ the quadrimomenta of the incoming and outgoing neutrinos, $\omega = E_\nu - E'_\nu$ and $\mathbf{q} = \mathbf{k} - \mathbf{k}'$, the energy and mo-

mentum transferred to the nucleus and θ the scattering angle. The $Z_0 N\Delta$ coupling can be extracted from the isovector piece of the spatial part of the $\bar{q}qZ_0$ vertex; with standard notation it reads

$$\begin{aligned} \mathcal{L}_{\bar{q}qZ_0} &= \frac{g_2}{2 \cos \theta_W} [V_\mu(x) - A_\mu(x)] Z_0^\mu(x) \\ &\simeq \frac{g_2}{2 \cos \theta_W} \bar{q}(x) \gamma_j (1 - \gamma_5) t_3^q q(x) Z_0^j(x). \end{aligned} \quad (1)$$

At low neutrino energy the dominant part is the hadronic axial current, i.e., the γ_5 piece. The vector current piece gives a relativistic correction which generates an axial-vector interference in the cross section, resulting in a higher cross section for neutrinos than for antineutrinos. For the single gamma production discussed below this interference gives typically a 30% effect compared with the averaged cross section where only the axial piece is taken into account. This point is discussed in some details in Sec. IV of Ref. [4] and is visible in Fig. 4 of Ref. [4], in Fig. 3 of Ref. [7], or in Figs. 5 and 8 of Ref. [8]. In this exploratory work devoted to the comparison of single gamma process with the pion exchange process we limit ourselves to the axial coupling such that, strictly speaking, our result applies to the average sum of the neutrino and antineutrino cross sections. Hence in the following we take:

$$\mathcal{L}_{\bar{q}qZ_0} \simeq -\frac{g_2}{2 \cos \theta_W} \bar{q}(x) \gamma_j \gamma_5 t_3^q q(x) Z_0^j(x). \quad (2)$$

The cross section for gamma production induced by a neutral current which excites a Delta from a nucleon with momentum p producing a photon in the final state writes:

$$\begin{aligned} d\sigma &= 2G_F^2 \frac{2\pi d \cos \theta k' E'_\nu dE'_\nu}{(2\pi)^3 2E_\nu 2E'_\nu} L_{\mu\eta} H^\mu H^{*\eta} 2\pi \delta \\ &\times (E_{f\gamma} + E'_\nu - E_p - E_\nu), \end{aligned} \quad (3)$$

with

$$\begin{aligned} L_{\mu\eta} &= \text{Tr}\{\not{k}\gamma_\mu(1-\gamma_5)\not{k}'\gamma_\eta(1-\gamma_5)\} \\ &= 8(k_\mu k'_\eta + k_\eta k'_\mu - g_{\mu\eta} k \cdot k' \pm i\varepsilon_{\mu\eta\alpha\beta} k^\alpha k'^\beta), \end{aligned} \quad (4)$$

$$H^\mu = \langle f\gamma | \int d\mathbf{x} \mathbf{j}_{em}(\mathbf{x}) \cdot \mathbf{A}(\mathbf{x}) | \Delta \rangle G_\Delta(\omega, \mathbf{p} + \mathbf{q}) \langle \Delta | \times | \int d\mathbf{y} \bar{q}(\mathbf{y}) \gamma^\mu \gamma_5 t_3^q q(\mathbf{y}) e^{i\mathbf{q}\cdot\mathbf{y}} | p \rangle. \quad (5)$$

The first form of the leptonic tensor applies to the neutrino case whereas the second form, with the explicit incorporation of the antisymmetric piece and where the plus (minus) sign refers to the neutrino (antineutrino), covers both ν and $\bar{\nu}$ cases. This antisymmetric piece, when contracted with the hadronic tensor, gives the axial-vector interference contribution to the cross section that we have ignored. For what concerns the hadronic piece H^μ , a summation over spin and isospin states of the intermediate delta is understood. For the Δ propagator, neglecting Fermi motion, we take the simplified form:

$$G_\Delta(\omega, \mathbf{q}) \simeq \left[\omega - \sqrt{M_\Delta^2 + q^2} + M_N + i \frac{\Gamma(\omega)}{2} \right]^{-1},$$

$$\Gamma(\omega) = \frac{1}{6\pi} \left(\frac{g_A}{2f_\pi} R_{N\Delta} \right)^2 (\omega^2 - m_\pi^2)^{3/2}, \text{ with } R_{N\Delta}$$

$$= \frac{g_{\pi N\Delta}}{g_{\pi NN}}. \quad (6)$$

In the numerical evaluations we take for the ratio of the Delta and nucleon coupling constants $R_{N\Delta} = 2$. As mentioned above, in the nonrelativistic limit the spatial part of the axial current dominates. We take it in the standard form:

$$\langle \Delta | \int d\mathbf{y} \bar{q}(\mathbf{y}) \gamma^j \gamma_5 t_3^q q(\mathbf{y}) e^{-i\mathbf{q}\cdot\mathbf{y}} | p \rangle = \frac{G_A [Q^2 = kk'(\cos\theta - 1)]}{2} R_{N\Delta} \langle \Delta | S_j T_3 | p \rangle, \quad (7)$$

where S_j (T_k) are the spin (isospin) transition operators between the spin-isospin $3/2\Delta$ state and the spin-isospin $1/2$ nucleon state with reduced matrix element $\langle \frac{3}{2} \| S, T \| \frac{1}{2} \rangle = 2$. On the right-hand side of Eq. (7) the Delta and proton states refer to the spin-isospin quantum numbers only. The axial form factor is taken in the standard dipole form with $G_A(0) = g_A = 1.26$ and a cutoff parameter $M_A = 1.032$ GeV.

II. SINGLE PHOTON EMISSION CROSS SECTIONS OFF NUCLEI

In the case of a single gamma emission (i.e., $\Delta \rightarrow \gamma N$) with momentum \mathbf{p}_γ and polarization $\vec{\epsilon}_\lambda$, the $\gamma N \Delta$ vertex, i.e., the electromagnetic matrix element, is obtained [15] by assuming the existence of a scaling law between the nucleon and Delta axial and magnetic matrix elements:

$$\langle N'(p'); \gamma(\mathbf{p}_\gamma, \vec{\epsilon}_\lambda) | \int d\mathbf{x} \mathbf{j}_{em}(\mathbf{x}) \cdot \mathbf{A}(\mathbf{x}) | \Delta \rangle = \frac{e}{\sqrt{2p_\gamma V}} \langle p' | \int d\mathbf{x} e^{-i\mathbf{p}'\cdot\mathbf{x}} \bar{q}(\mathbf{x}) \vec{\gamma} \cdot \vec{\epsilon} \left(\frac{1}{6} + t_3^q \right) q(\mathbf{x}) | \Delta \rangle$$

$$= -\frac{ieR_{N\Delta}}{\sqrt{2p_\gamma V}} \frac{\mu_p - \mu_n}{4M_N} \langle p' | (\mathbf{S}^\dagger \times \mathbf{p}_\gamma) \cdot \vec{\epsilon} T_3^\dagger | \Delta \rangle \delta_{\mathbf{p}_\gamma + \mathbf{p}' - \mathbf{q} - \mathbf{p}}. \quad (8)$$

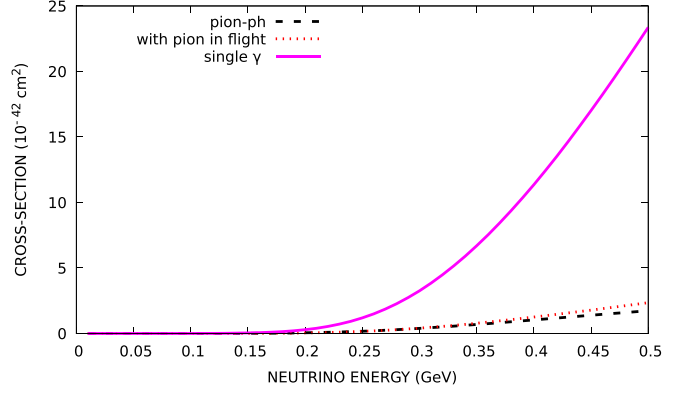


FIG. 2. Full line shows single γ cross section for ^{12}C [graph of Fig. 1(a)] in 10^{-42} cm 2 versus neutrino energy in GeV. Dashed line shows γ -pion-ph cross section for ^{12}C with only the contact term [graph of Fig. 1(b)]. Dotted line shows γ -pion-ph cross section with inclusion of the pion in flight process [graphs of Figs. 1(b) and 1(c)].

(9)

In the evaluation of the cross section, one has to perform a summation over the spin-isospin states of the intermediate Delta and of the final emitted nucleon (see Appendix). Ignoring Fermi motion, the resulting cross section per nucleon for gamma production writes:

$$\frac{d\sigma^\gamma}{dE'_\nu d\cos\theta} = \left[\frac{G_F^2 k'}{4\pi} 8kk'(3 - \cos\theta) \right] \times \left[\frac{4}{9} R_{N\Delta}^2 \left(\frac{G_A(Q^2)}{2} \right)^2 \right] \left[\frac{1}{2\pi} \Gamma^\gamma(\omega) \right]. \quad (10)$$

Neglecting nucleon recoil, the radiative Delta width $\Gamma^\gamma(\omega)$ is

$$\Gamma^\gamma(\omega) = \frac{4}{9} R_{N\Delta}^2 \left(\frac{e}{2M_N} \right)^2 \left(\frac{\mu_p - \mu_n}{2} \right)^2 \times \int \frac{d\mathbf{p}_\gamma}{(2\pi)^3 2p_\gamma} p_\gamma^2 2\pi \delta(p_\gamma + \epsilon_p - \omega - \epsilon_p)$$

$$\simeq \frac{4}{9} R_{N\Delta}^2 \left(\frac{e}{2M_N} \right)^2 \left(\frac{\mu_p - \mu_n}{2} \right)^2 \frac{\omega^3}{2\pi}. \quad (11)$$

The result of our evaluation for the single gamma emission off ^{12}C as a function of the neutrino energy is displayed on Fig. 2. We find a qualitative agreement with Refs. [4–9], certainly not perfect but sufficient for the purpose of this article. For instance, for a neutrino energy of $E_\nu = 0.3$ GeV, we find for the cross section per nucleon $\sigma^\gamma/A \simeq 0.27 \times 10^{-42}$ cm 2 , which is twice larger than the Delta contribution shown in Fig. 4 of Ref. [4], but the cut of 200 MeV applied to the photon energy in this reference could explain this difference. For a neutrino energy of $E_\nu = 0.5$ GeV, we find $\sigma^\gamma/A \simeq 2 \times 10^{-42}$ cm 2 which is close, although slightly larger, to the averaged $\nu\bar{\nu}$ cross section shown in the same figure (Fig. 4 of Ref. [4]) and in Fig. 8 of Ref. [8]. Here it is apparent that this Delta contribution dominates over other processes such as “Compton-like” scattering and omega exchange. At a higher neutrino energy, $E_\nu = 1$ GeV, we find $\sigma^\gamma/A \simeq 8 \times 10^{-42}$ cm 2 , again slightly larger than the averaged $\nu\bar{\nu}$ cross

section obtained in Refs. [4,7,8] where it is apparent that the Delta contribution is largely dominant.

III. PHOTON-PION EMISSION CROSS SECTIONS OFF NUCLEI

As mentioned previously the specific realization of chiral symmetry in the hadronic world implies that, for any process involving a vector correlator there is an associated axial correlator process through the emission or the absorption of an s -wave pion; this is referred to as the axial-vector correlator mixing effect. This mixing implies that there is a $N\Delta\gamma\pi$ vertex associated with the direct $N\Delta\gamma$ vertex. There are several ways to derive this vertex. One is to start from an effective chiral theory formulated at the quark level [16] or more directly at the nucleonic level (see Ref. [17] for a recent review). In both cases the Goldstone pion field $\vec{\phi}(x)$ is introduced through a matrix $U(x) = e^{i\vec{\tau}\cdot\vec{\phi}(x)/f_\pi}$ having a perfectly well defined transformation law under chiral rotations. Nucleons can be also introduced as heavy sources coupled to pions [18]. The leading term is dictated by chiral symmetry alone:

$$\begin{aligned} \mathcal{L}_N^{(1)} &= \bar{\psi}_N [i\gamma_\mu(\partial^\mu + iv^\mu) + g_A\gamma_\mu\gamma^5 a^\mu - M_N] \psi_N \\ &\simeq \bar{\psi}_N (i\gamma_\mu\partial^\mu - M_N) - \frac{g_A}{2f_\pi} \bar{\psi}_N \gamma_\mu \gamma^5 \vec{\tau} \psi_N \cdot \partial^\mu \vec{\phi} \\ &\quad - \frac{1}{4f_\pi^2} \bar{\psi}_N \gamma_\mu \vec{\tau} \psi_N \cdot \vec{\phi} \times \partial^\mu \vec{\phi} \\ \text{with } \xi &= \sqrt{U}, \quad v^\mu = \frac{i}{2} (\xi \partial^\mu \xi^\dagger + \xi^\dagger \partial^\mu \xi), \\ a^\mu &= \frac{i}{2} (\xi \partial^\mu \xi^\dagger - \xi^\dagger \partial^\mu \xi), \end{aligned} \quad (12)$$

where the Dirac spinor ψ_N denotes the iso-doublet of nucleons. There are two parameters which are not determined by chiral symmetry: the nucleon mass (in principle in the chiral limit M_0) and the axial coupling constant, $g_A = 1.26$, known from the analysis of neutron beta decay. The coupling to the electromagnetic field is simply obtained by gauging the above Lagrangian by the appropriate minimal substitution:

$$\partial^\mu \xi \rightarrow \partial^\mu \xi + ie \frac{1 + \tau_3}{2} A^\mu \xi,$$

$$\partial^\mu \xi^\dagger \rightarrow \partial^\mu \xi^\dagger + ie \frac{1 + \tau_3}{2} A^\mu \xi^\dagger. \quad (13)$$

This generates the following Lagrangian:

$$\begin{aligned} \mathcal{L}_{NN\gamma\pi} &= -\frac{e}{2} g_A A_\mu \bar{\psi}_N \gamma_\mu \gamma^5 \left(\xi \frac{\tau_3}{2} \xi^\dagger - \xi^\dagger \frac{\tau_3}{2} \xi \right) \psi_N \\ &\simeq -e g_A A_\mu \bar{\psi}_N \gamma_\mu \gamma^5 \frac{\vec{\tau}}{2f_\pi} \cdot (\vec{e}_3 \times \vec{\phi}) \psi_N \\ &= -ie \frac{g_A}{2f_\pi} A_\mu \bar{\psi}_N \gamma_\mu \gamma^5 (\tau_+^\dagger \phi_+ + \tau_-^\dagger \phi_-) \psi_N \\ \text{with } \tau_\pm &= \mp \frac{\tau_1 \pm i\tau_2}{\sqrt{2}}, \quad \phi_\pm = \frac{\phi_1 \pm \phi_2}{\sqrt{2}}, \text{ creating a } \pi^\pm. \end{aligned} \quad (14)$$

Hence the matrix element of the electromagnetic interaction between an initial nucleon and a final state made of a nucleon, a photon and a charged pion π^α reads:

$$\begin{aligned} &\langle N'(p'); \gamma(\mathbf{p}_\gamma, \vec{\epsilon}_\lambda); \pi^\alpha(\mathbf{p}_\pi) | \int d\mathbf{x} \mathbf{j}_{em}(\mathbf{x}) \cdot \mathbf{A}(\mathbf{x}) | N \rangle \\ &= \frac{e}{\sqrt{2p_\gamma V 2E_\pi V}} \frac{g_A}{2f_\pi} \langle p' | \\ &\quad \times \int d\mathbf{x} e^{-i(\mathbf{p}_\gamma + \mathbf{p}_\pi) \cdot \mathbf{x}} \bar{\psi}_N(\mathbf{x}) \gamma_\mu \gamma^5 \tau_\alpha^\dagger \psi_N(\mathbf{x}) | N \rangle \\ &\simeq \frac{e}{\sqrt{2p_\gamma V 2E_\pi V}} \frac{g_A}{2f_\pi} \langle p' | \vec{\sigma} \cdot \vec{\epsilon}_\lambda \tau_\alpha^\dagger | N \rangle \delta_{\mathbf{p}_\gamma + \mathbf{p}_\pi + \mathbf{p}' - \mathbf{q} - \mathbf{p}}, \end{aligned} \quad (15)$$

where in the nonrelativistic approximation of the last line the nucleon states refer to the spin-isospin quantum numbers only. The extension to the $N\Delta\gamma\pi$ vertex is straightforward with the replacement of the Pauli matrices by the spin and isospin transition operators with the same rescaling of the coupling constants as previously:

$$\langle N'(p'); \gamma(\mathbf{p}_\gamma, \vec{\epsilon}_\lambda); \pi^\alpha(\mathbf{p}_\pi) | \int d\mathbf{x} \mathbf{j}_{em}(\mathbf{x}) \cdot \mathbf{A}(\mathbf{x}) | \Delta \rangle = \frac{e}{\sqrt{2p_\gamma V 2E_\pi V}} R_{N\Delta} \frac{g_A}{2f_\pi} \langle p' | \mathbf{S}^\dagger \cdot \vec{\epsilon}_\lambda T_\alpha^\dagger | \Delta \rangle \delta_{\mathbf{p}_\gamma + \mathbf{p}_\pi + \mathbf{p}' - \mathbf{q} - \mathbf{p}}. \quad (16)$$

After performing again the spin-isospin summation over intermediate delta and final emitted nucleon, we obtain for the photon-pion production cross section:

$$\frac{d\sigma^{\gamma\pi}}{dE'_d d\cos\theta} = \left[\frac{G_F^2 k'}{4\pi k} 8kk'(3 - \cos\theta) \right] \left[\frac{4}{9} R_{N\Delta}^2 \left(\frac{G_A(Q^2)}{2} \right)^2 \right] \left[\frac{1}{2\pi} \Gamma^{\gamma\pi}(\omega) \right]. \quad (17)$$

The radiative Delta-pion width is

$$\begin{aligned} \Gamma^{\gamma\pi}(\omega) &= e^2 \frac{2}{9} R_{N\Delta}^2 \left(\frac{g_A}{2f_\pi} \right)^2 \int \frac{d\mathbf{p}_\gamma}{(2\pi)^3 2p_\gamma} \int \frac{d\mathbf{p}_\pi}{(2\pi)^3 2E_\pi} 2\pi \delta(p_\gamma + E_\pi + \epsilon_{p'} - \omega - \epsilon_p) \\ &\simeq \frac{e^2}{(2\pi)^3} \frac{2}{9} R_{N\Delta}^2 \left(\frac{g_A}{2f_\pi} \right)^2 \int_0^\infty dp_\gamma p_\gamma \int_{m_\pi}^\infty dE_\pi p_\pi \delta(p_\gamma + E_\pi - \omega) \\ &\simeq \frac{e^2}{(2\pi)^3} \frac{2}{9} R_{N\Delta}^2 \left(\frac{g_A}{2f_\pi} \right)^2 \int_0^\infty dp_\gamma p_\gamma \int_{m_\pi}^\infty dE_\pi p_\pi \left(-\frac{2E_\pi}{\pi} \right) \text{Im} D_{0\pi}(\omega - p_\gamma, p_\pi = \sqrt{E_\pi^2 - m_\pi^2}). \end{aligned} \quad (18)$$

In the last two expressions nucleon recoils have been neglected. The in-medium cross-section is obtained by replacing the bare pion propagator by the in-medium pion propagator according to

$$\text{Im}D_{0\pi}(\Omega, p_\pi) = \text{Im}[\Omega^2 - m_\pi^2 - p_\pi^2 + i\eta]^{-1} \rightarrow \text{Im}D_\pi(\Omega, p_\pi) = \text{Im}[\Omega^2 - m_\pi^2 - p_\pi^2 - S(\Omega, p_\pi)]^{-1}, \quad (19)$$

where $S(\Omega, p_\pi)$ is the irreducible pion self-energy. This quantity receives contributions from particle-hole and Delta-hole states corrected by short-range screening effects described by three Landau-Migdal parameters [19]: $g'_{NN} = 0.7$, $g'_{N\Delta} = 0.5$, $g'_{\Delta\Delta} = 0.3$, according to:

$$S(\Omega, p_\pi) = p_\pi^2 \tilde{\Pi}_0(\Omega, p_\pi) = p_\pi^2 \frac{\Pi_{0N} + \Pi_{0\Delta} + (2g'_{NN} - g'_{N\Delta} - g'_{\Delta\Delta})\Pi_{0N}\Pi_{0\Delta}}{(1 - g'_{NN}\Pi_{0N})(1 - g'_{\Delta\Delta}\Pi_{0\Delta}) - g'^2_{N\Delta}\Pi_{0N}\Pi_{0\Delta}}, \quad (20)$$

with

$$\Pi_{0N}(\Omega, p_\pi) = 4 \left(\frac{g_A}{2f_\pi} \right)^2 v^2(p_\pi) \int \frac{d\mathbf{h}}{(2\pi)^3} \left(\frac{\Theta(p_F - h)\Theta(|\mathbf{h} + \mathbf{p}_\pi| - p_F)}{\Omega - \epsilon_{\mathbf{h}+\mathbf{p}_\pi} + \epsilon_h + i\eta} - \frac{\Theta(p_F - h)\Theta(|\mathbf{h} - \mathbf{p}_\pi| - p_F)}{\Omega + \epsilon_{\mathbf{h}-\mathbf{p}_\pi} - \epsilon_h - i\eta} \right), \quad (21)$$

$$\Pi_{0\Delta}(\Omega, \mathbf{p}_\pi) = \frac{16}{9} R_{N\Delta}^2 \left(\frac{g_A}{2f_\pi} \right)^2 v^2(p_\pi) \int \frac{d\mathbf{h}}{(2\pi)^3} \Theta(p_F - h) \left(\frac{1}{\Omega - \epsilon_{\Delta, \mathbf{h}+\mathbf{p}_\pi} + \epsilon_h + i\Gamma_\Delta(\Omega, \mathbf{h} + \mathbf{p}_\pi)} - \frac{1}{\Omega + \epsilon_{\Delta, \mathbf{h}-\mathbf{p}_\pi} - \epsilon_h} \right). \quad (22)$$

$v(p_\pi)$ is a dipole πNN form factor with cutoff $\Lambda = 0.98$ GeV, as in our previous works [20,21]. For the imaginary part of the in-medium pion propagator we select only those contributions coming from the dressing of the pion propagator by particle-hole states [see Fig. 1(b)]. Hence the pion produced is disguised as p-h states which are invisible in the MiniBoone detector. This simulates a simple gamma process and contributes to an increase of the gamma emission from the Delta decay. The radiative delta-pion width entering the cross section [Eq. (17)] thus takes the form

$$\Gamma^{\gamma\pi(ph)}(\omega) \simeq \frac{e^2}{(2\pi)^3} \frac{2}{9} R_{N\Delta}^2 \left(\frac{g_A}{2f_\pi} \right)^2 \int_0^\infty dp_\gamma p_\gamma \int_{m_\pi}^\infty dE_\pi p_\pi \frac{(-\frac{2E_\pi}{\pi}) p_\pi^2 \text{Im}\tilde{\Pi}_0(\omega - p_\gamma, p_\pi = \sqrt{E_\pi^2 - m_\pi^2})}{|(\omega - p_\gamma)^2 - m_\pi^2 - p_\pi^2 - p_\pi^2 \tilde{\Pi}_0(\omega - p_\gamma, p_\pi)|^2}. \quad (23)$$

In the relevant energy domain only the ph bubble has an imaginary part:

$$\text{Im}\Pi_{0N}(\Omega, \mathbf{p}_\pi) = -4\pi \left(\frac{g_A}{2f_\pi} \right)^2 v^2(p_\pi) \int \frac{d\mathbf{h}}{(2\pi)^3} \Theta(p_F - h)\Theta(|\mathbf{h} + \mathbf{p}_\pi| - p_F)\delta(\Omega - \epsilon_{\mathbf{h}+\mathbf{p}_\pi} + \epsilon_h). \quad (24)$$

The inclusion of the pion in flight term [Fig. 1(c)] can be achieved by modifying the contact vertex spin operator $\mathbf{S}^\dagger \cdot \vec{\epsilon}_\lambda$ appearing in Eq. (16) according to [22]

$$\mathbf{S}^\dagger \cdot \vec{\epsilon}_\lambda \rightarrow \mathbf{S}^\dagger \cdot \vec{\epsilon}_\lambda - \frac{2\mathbf{S}^\dagger \cdot \mathbf{t} \cdot \vec{\epsilon}_\lambda}{T^2 + m_\pi^2}, \quad (25)$$

where \mathbf{t} and t_0 are the momentum and energy ($T^2 = t^2 - t_0^2$) of the flying pion. After summation over the photon polarization states and averaging over the photon momentum direction, the net effect is the presence in the integrant of $\Gamma^{\gamma\pi}(\omega)$ in Eq. (18) of a correction factor F_{Flight} given by

$$F_{\text{Flight}} = 1 + \frac{4}{3} \frac{t^2}{T^2 + m_\pi^2} \left(\frac{t^2}{T^2 + m_\pi^2} - 1 \right). \quad (26)$$

If we assume the nucleon recoil momentum to average to zero, we can replace the momentum \mathbf{t} of the flying pion by the momentum \mathbf{q} transferred by the neutrino. As the nuclear response is limited to the low-energy domain we can replace the energy t_0 of the flying pion by the photon energy p_γ . The result of the calculation for the photon-pion emission cross section without and with the pion in flight terms are shown in Fig. 2. In Fig. 3 we show their ratio with the single gamma cross section.

We have also looked at the 2p-2h absorption mode of the exchanged pion, the dominant mode for physical pions, which

would also lead to a simulation of electron rings. This is achieved by adding to the polarization bubbles $\Pi_{0N,\Delta}(\omega - p_\gamma, \mathbf{p}_\pi)$ [Eq. (21)] a purely imaginary piece. According to previous studies [13,21], we approximate it as linearly growing in the low-energy domain, i.e., $\omega - p_\gamma < m_\pi$:

$$\Pi_{02p2h}(\omega - p_\gamma, \mathbf{p}_\pi) = -i4\pi \text{Im}C_0 \rho^2 \left(\frac{\omega - p_\gamma}{m_\pi} \right), \quad (27)$$

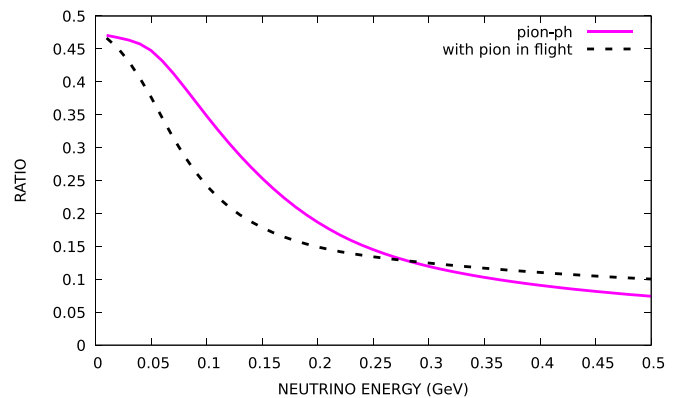


FIG. 3. Ratio of the γ -pion-ph and single γ cross sections versus neutrino energy in GeV without (full line) and with (dashed line) the pion in flight process of Fig. 1(c).

with $\text{Im } C_0 = 0.13m_\pi^{-6}$ so as to reproduce the absorptive part of the pion-nucleus optical potential. For $\omega - p_\gamma > m_\pi$ we keep it constant up to a maximum value of 400 MeV for $\omega - p_\gamma > m_\pi$ and zero beyond.

IV. DISCUSSION

We show in Fig. 2 the results of the calculation of the cross section for single gamma emission and for gamma-virtual pion-ph emission. We also display the result of our calculation when the pion in flight process [Fig. 1(c)] is introduced on top of the contact term of Fig. 1(b). Up to a neutrino energy of about 0.3 GeV the pion in flight contribution is opposite to that of the contact term. In Figs. 3 and 4 we display the ratio between the gamma-pion and single gamma cross sections without and with the 2p-2h absorption mode of the virtual pion. The comparison of these two figures shows that the effect of this mode is moderate.

In conclusion, the exchange process that we have introduced is smaller than the single gamma process but nevertheless significant. Here we have considered only the emission from a $N\Delta\gamma$ vertex. Other similar meson exchange terms may also be at work through more complex pion emission processes. Their complete evaluation should be done before a definite conclusion can be drawn about the real importance of gamma rings simulating electron rings production by neutrinos, which could affect some conclusions about the sterile neutrinos.

Finally, recall that our evaluation is restricted to the influence of the pion exchange effects on the average of the

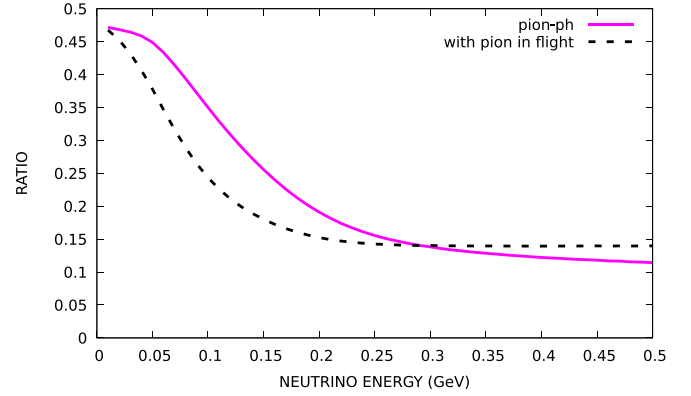


FIG. 4. The same as Fig. 3 but with the inclusion of the 2p-2h contribution in the pion self-energy.

neutrino and antineutrino cross sections. The investigation into the influence of their difference, which is relevant for CP violation, will be the object of future work.

APPENDIX: DETAILS FOR THE CALCULATION OF THE SINGLE GAMMA CROSS SECTION

The calculation of the single gamma cross section involves the axial vector matrix element [Eq. (7)] and the electromagnetic matrix element [Eq. (9)]. When re-injected in the expression of the cross section [Eq. (3)], this requires a summation over the spin-isospin states of the intermediate Delta and of the final emitted nucleon according to

$$\begin{aligned}
& \sum_{M'_S, M'_T} \sum_{M_S, M_T} \sum_{\lambda} \sum_{j, k} \langle p : m_s, m_t | S_j^\dagger T_3^\dagger | M'_S, M'_T \rangle \int \frac{d\hat{p}_\gamma}{4\pi} \sum_{m'_s, m'_t, \lambda} \langle M'_S, M'_T | (\mathbf{S} \times \mathbf{p}_\gamma) \cdot \vec{\epsilon}_\lambda T_3 | m'_s, m'_t \rangle \\
& \langle m'_s, m'_t | (\mathbf{S}^\dagger \times \mathbf{p}_\gamma) \cdot \vec{\epsilon}_\lambda T_3^\dagger | M_S, M_T \rangle \langle M_S, M_T | S_k T_3 | p : m_s, m_t \rangle L^{jk} \\
& = \sum_{M'_S, M'_T} \sum_{M_S, M_T} \sum_{j, k} \langle p : m_s, m_t | S_j^\dagger T_3^\dagger | M'_S, M'_T \rangle \int \frac{d\hat{p}_\gamma}{4\pi} p_\gamma^2 \frac{4}{9} \delta_{M_S, M'_S} \delta_{M_T, M'_T} \langle M'_S, M'_T | S_k T_3 | p : m_s, m_t \rangle L^{jk} \\
& = \int \frac{d\hat{p}_\gamma}{4\pi} \frac{4p_\gamma^2}{9} \langle p : m_s, m_t | \left(\frac{2}{3} \delta_{jk} - \frac{i}{3} \epsilon_{jkl} \sigma_l \right) \frac{2}{3} | p : m_s, m_t \rangle L^{jk} = \int \frac{d\hat{p}_\gamma}{4\pi} \frac{4p_\gamma^2}{9} \frac{4}{9} (L^{11} + L^{22} + L^{33}) \\
& = \int \frac{d\hat{p}_\gamma}{4\pi} \frac{4p_\gamma^2}{9} \frac{4}{9} [8kk'(3 - \cos \theta)]. \tag{A1}
\end{aligned}$$

Grouping all the terms together, the cross section per nucleon for gamma production given in Eq. (10) follows

- [1] A. Aguilar-Arevalo *et al.* (MiniBoone Collaboration), *Phys. Rev. Lett.* **102**, 101802 (2009).
[2] A. Aguilar-Arevalo *et al.* (MiniBoone Collaboration), *Phys. Rev. Lett.* **110**, 161801 (2013).
[3] A. Aguilar-Arevalo *et al.* (MiniBoone Collaboration), *Phys. Rev. Lett.* **121**, 221801 (2018).
[4] R. J. Hill, *Phys. Rev. D* **81**, 013008 (2010).
[5] R. J. Hill, *Phys. Rev. D* **84**, 017501 (2011).
[6] B. D. Serot and X. Zhang, *Phys. Rev. C* **86**, 015501 (2012).
[7] X. Zhang and B. D. Serot, *Phys. Lett. B* **719**, 409 (2013).
[8] E. Wang, L. Alvarez-Ruso, and J. Nieves, *Phys. Rev. C* **89**, 015503 (2014).
[9] E. Wang, L. Alvarez-Ruso, and J. Nieves, *Phys. Lett. B* **740**, 16 (2015).
[10] T. Katori (MiniBooNE Collaboration), [arXiv:2010.06015](https://arxiv.org/abs/2010.06015) [hep-ex].

- [11] G. Chanfray, J. Delorme, M. Ericson, and M. Rosa-Clot, *Phys. Lett. B* **455**, 39 (1999).
- [12] M. Dey, V. L. Eletsky, and B. L. Ioffe, *Phys. Lett. B* **252**, 620 (1990).
- [13] G. Chanfray and P. Schuck, *Nucl. Phys. A* **555**, 329 (1993).
- [14] G. Chanfray, R. Rapp, and J. Wambach, *Phys. Rev. Lett.* **76**, 368 (1996); *Nucl. Phys. A* **617**, 472 (1997).
- [15] E. Oset, H. Toki, and W. Weise, *Phys. Rep.* **83**, 281 (1982).
- [16] F. Belleman, A. Berg, J. Bisplinghoff, G. Bohlscheid, J. Ernst, C. Henrich, F. Hinterberger, R. Ibal, R. Jahn, R. Joosten, K. Kilian, A. Kozela, H. Machner, A. Magiera, J. Munkel, P. von Neumann-Cosel, P. von Rossen, H. Schnitker, K. Scho, J. Smyrski, R. Tolle, and C. Wilkin, *Phys. Rev. C* **75**, 015204 (2007).
- [17] W. Holt, M. Rho, and W. Weise, *Phys. Rep.* **621**, 2 (2016).
- [18] V. Bernard, N. Kaiser, and U.-G. Meißner, *Int. J. Mod. Phys. E* **4**, 193 (1995).
- [19] M. Ichimura, H. Sakai, and T. Wakasa, *Prog. Part. Nucl. Phys.* **56**, 446 (2006).
- [20] G. Chanfray and M. Ericson, *Phys. Rev. C* **75**, 015206 (2007).
- [21] M. Martini, M. Ericson, G. Chanfray, and J. Marteau, *Phys. Rev. C* **80**, 065501 (2009).
- [22] G. Chanfray and J. Delorme, *Phys. Lett. B* **129**, 167 (1983); G. Chanfray, *Nucl. Phys. A* **429**, 489 (1984).